Chalcogen bonding interactions in chelating, chiral bis(selenocyanates)

Huu-Tri Huynh, Olivier Jeannin, Emmanuel Aubert, Enrique Espinosa, Marc Fourmigue

Chalcogen bonding interactions in chelating, chiral bis(selenocyanates)†

Huu-Tri Huynh,[a] Olivier Jeannin,[a] Emmanuel Aubert,[b] Enrique Espinosa[b] and Marc Fourmigué*[a]

[a]*Univ Rennes, CNRS, ISCR (Institut des Sciences Chimiques de Rennes) - UMR 6226, F-35000 Rennes, France. E-mail: marc.fourmigue@univ-rennes1.fr*

[b] *Université de Lorraine, CNRS, CRM2 , F-54000 Nancy, France*

† Electronic supplementary information (ESI) available: Computational details. CCDC 2040289-2040296. For ESI and crystallographic data in cif or other electronic format see DOI: 10.1039/XXXXXX

Abstract

Introduction of methyl substituents on the achiral 1,2-bis(selenocyanatomethyl)benzene leads to a novel chelating ChB donor, namely 1,2-bis(1-selenocyanatoethyl)benzene (**1**), as a mixture of three diastereomers, the two *anti* enantiomers and the *syn* (*meso*) form. Structure determinations show the recurrent formation of short Se•••N≡C ChB interactions in both the *anti* (racemic mixture) and *syn* isomers. Co-crystallization of *anti*-**1** with 4,4'-bipyridine affords a 2:1 adduct, (*anti*-**1**)$_2$(bipy), with one very short Se•••N$_{Py}$ ChB (RR = 0.87). Co-crystallization of *anti*-**1** with tetraphenylphosphonium halides (Cl^-, Br^-, I^-) provides 1:1 adducts while a 2:1 adduct is isolated between *syn*-**1** and Et_4NCl, formulated as $Et_4N^+[(syn\text{-}\mathbf{1})_2Cl^-]$. Comparison of chloride chelation with *anti*-**1** and *syn*-**1** shows much shorter (NC)Se•••Cl^- ChB interactions with the *syn* isomer, tentatively rationalized on the basis of theoretical calculations of (i) the electrostatic surface potential of neutral ChB donors and (ii) the chloride BSSE complexation energy.

Introduction

Non-covalent interactions[1] are currently developing as a cross-field area encompassing many different topics found in crystal engineering, anion recognition and transport, catalysis, biochemistry, material science. Following the huge development of halogen bonding (XB) in the last 25 years,[2] it became clear that elements of group 14, 15 and 16 of the periodic table were also prone to exhibit electrophilic sites prone to interact with charge-concentrated area, in a way very similar to that shown by halogens where the development of an electron-deficient region (also called sigma-hole)[3] in the prolongation of the covalent bond to the halogen allows for strong and directional interactions with Lewis bases. These newcomers to the field, described as tetrel (TrB),[4] pnictogen (PnB)[5] and chalcogen bonds (ChB),[6] albeit much less developed than XB, present some specificities and offer new possibilities particularly on the field of supramolecular self-assembly and crystal engineering,[6a,7] catalysis,[8] anion recognition[9] and transport,[10] biochemistry.[11] If we focus on ChB, one main difference with XB is the presence, on the chalcogen atom when properly activated, of not one but two electron-depleted regions, located approximately in the extension of the two covalent bonds to the chalcogen.[3,12,13] This added element of complexity has several important structural implications such as: (i) possible deviations between the C_i–Ch and Ch•••X (X = Lewis base) axes, and (ii) possibility for dissymmetry of chalcogen substitution implying a dissymmetry of the two σ-hole area. As a consequence, the very strong predictability of XB interactions finds in the analogous ChB systems some limitations, which have hampered its extensive use in crystal engineering strategies. Several prominent examples have however successfully overcome these problems, such as the self-assembly of 1,2-tellurazole 2-oxides into a variety of supramolecular aggregates,[14] the use of bis-(selenophene/tellurophene) derivatives as chelating systems toward anions (Scheme 1a),[10,15,16] or double chalcogen bonding interactions exhibited by benzo-1,3-chalcogenazoles[17] or chalcogenadiazoles.[18]

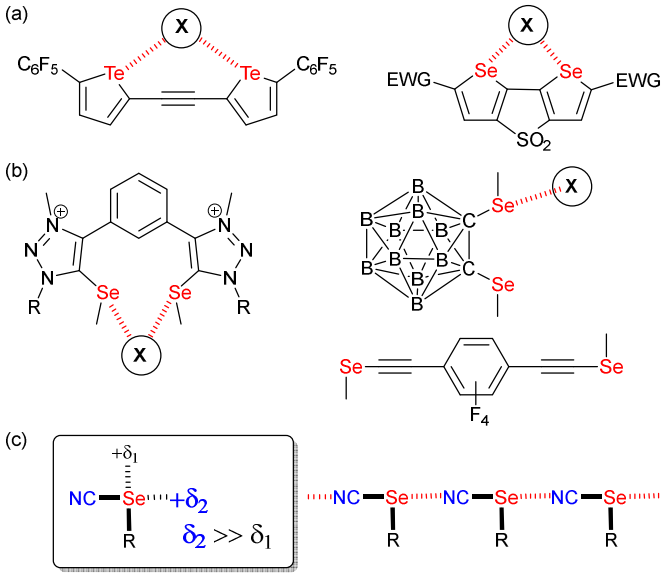

Scheme 1 (a) Structures of reported ChB donors chelating halides. (b) Systems with strongly asymmetric selenium activation (c) Organic selenocyanates: sigma-holes and solid-state association.

Along these lines, one attempt to restore in ChB systems the strong directionality offered by halogens consists in functionalizing the chalcogen atom with only one strong electron-withdrawing substituent, as for example in rotaxanes incorporating selenomethyltriazolium moieties,[19] in selenomethyl- or tellluromethyl-acetylenes,[20] in icosahedral *ortho*-carboranes substituted with two methylseleno or methyltelluro groups (Scheme 1b),[21] or in selenocyanate derivatives R–SeCN (Scheme 1c).[22,23] In such compounds, the electron-withdrawing character of the nitrile substituents strongly activates one of the two σ-holes, in the prolongation of the NC–Se bond, allowing to recover the predictability of interaction with Lewis bases. Indeed, selenocyanates themselves most often crystalize into chains •••NC–(R)Se•••NC–(R)Se••• where the lone pair of the nitrogen atom of the nitrile interacts through ChB with the selenium atom with Se•••N distances around 3.0 Å, that is a reduction ratio RR (defined as the actual interatomic distance over the sum of the van der Waals radii) around 0.86. Recently, we reported several *bis*- or *tetrakis*-substituted selenocyanate derivatives such as A-D in Scheme 2a,[23] easily prepared from the corresponding benzylic bromides and KSeCN, which were shown to organize in the solid state with these recurrent chain-like motifs. These ChB interactions are notably enhanced when the selenocyanate is faced with stronger Lewis bases such as pyridines[24] or halide anions.[25] A remarkable feature of the *ortho* derivative A (or the 1,2,4,5-*tetrakis* derivative D) is its ability to chelate one single atom through the two selenium atoms, giving rise to seven-membered rings with either neutral (DMF) or anionic (halides) Lewis bases

(Scheme 2b). These interactions were also confirmed in solution by ^{13}C and ^{77}Se NMR.[26] With the ChB donors A and D, two specific conformations of the *ortho*-selenocyanatomethyl arms were observed on the solid state upon halide chelation, namely *syn* or *anti*, depending on the halide anion, its coordination number and the associated counter ion, without possibility to evaluate the relative stability of both conformations. In order to clarify this point and possibly favor one over the other conformation in these halide recognition processes, we designed an *ortho* bis(selenocyanate) derivative **1** analogous to A, but bearing an extra methyl group on each benzylic bridge (Scheme 2c). Compound **1** does thus exist as three diastereomers, the two *anti* enantiomers and the *syn* (*meso*) form. We describe here its synthesis, separation of the *anti* and *syn* forms and their association with neutral (4,4'-bipyridine) and charged (halide anion) Lewis bases. This novel ChB donor provides also a rare example of introduction of chirality in chalcogen-bonded systems.[27] Indeed, only a few examples of selenylation reagents were reported where an intramolecular Se•••N or Se•••O interaction rigidifies the chiral reagent and thus allows for stereochemical control,[6c,28] while recently a planar chiral ferrocenyl plateform was functionalized with iodomethyl- and selenomethyl-ethynyl moieties[29] for evaluation in the Ritter reaction.[30]

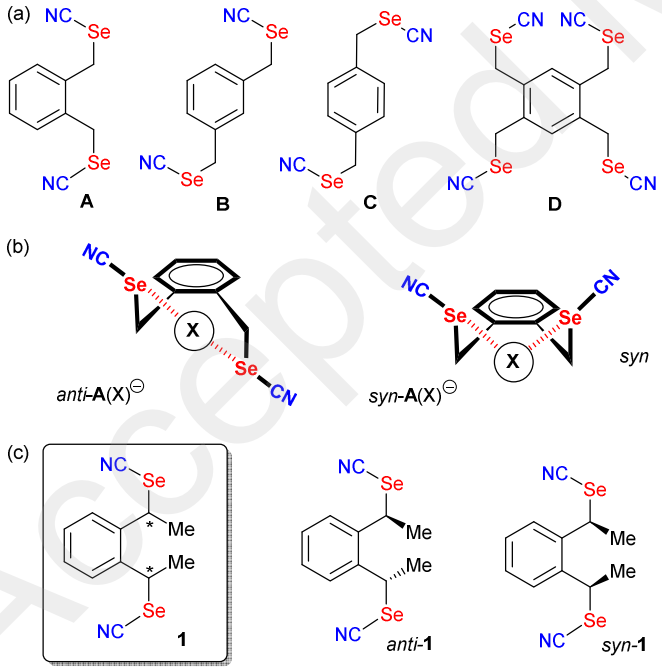

Scheme 2 Benzylic selenocyanates and their halide chelates.

Results and discussion

Syntheses. The preparation of **1** is based on the nucleophilic substitution of 1,2-bis(1-bromoethyl)benzene **2** with KSeCN (Scheme 3). The preparation of **2** from reaction of 1,2-diethylbenzene with NBS has been reported to afford a diastereoisomeric mixture in a 3:1 ratio.[31] Recrystallization was reported to yield a crystalline material composed essentially of the majority compound, whose stereochemistry was not assigned at that time. Based on the product obtained from the majority dibromo compound when reacted with glycine,[32] the main diastereoisomer was later shown to be the *anti* one.

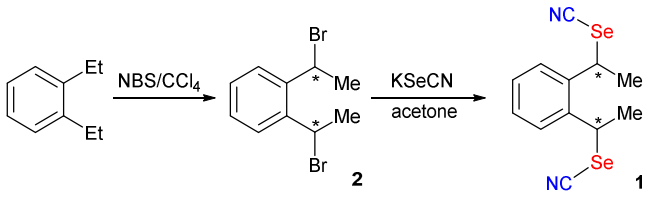

Scheme 3. Synthetic path to **1**.

We have performed the bromination reaction of 1,2-diethylbenzene in the same conditions and isolated indeed a 70:30 *anti-syn* mixture. Recrystallization from hexane afforded the pure *anti* isomer whose stereochemistry was confirmed here by single crystal X-ray diffraction. Concentration of the mother liquors gives a 23:77 *anti-syn* mixture based on NMR. The dibromo derivative *anti*-**2** crystallizes in the monoclinic system, S. G. $P2_1/n$ with one molecule in general position (Figure 1a). No short intermolecular Br•••Br are identified. Nucleophilic substitution with KSeCN was not stereochemically conservative and afforded a mixture of *anti*- and *syn*-**1**, in 3:1 ratio when performed from pure *anti*-**2**. Recrystallization from acetone allowed to isolate *anti*-**1** in a pure form. It crystallizes in the monoclinic system, S. G. $P2_1/a$ with one molecule in general position (Figure 1b) together with one of the SeCN moieties disordered on two positions with 60:40 refined occupancy. From the concentrated mother liquors, some crystals of *syn*-**1** were isolated with difficulties after hexane diffusion. The *syn* isomer was found to crystallize in the monoclinic system, S. G. $P2_1/c$ with one molecule in general position (Figure 1c).

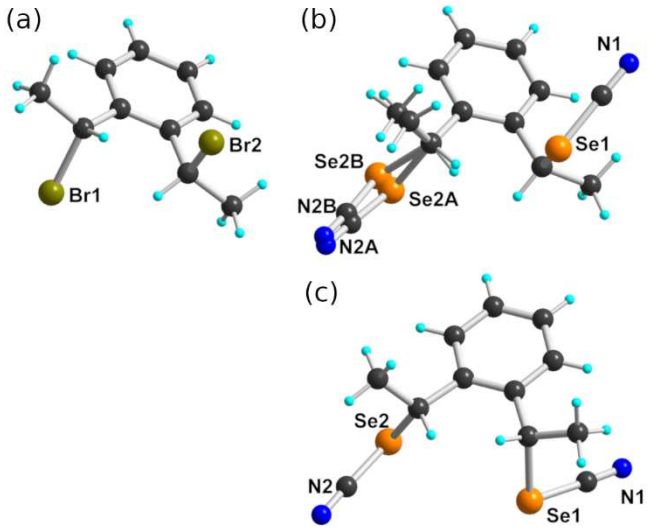

Fig. 1 Detail of the molecular structures of (a) *anti*-**2**, (b) *anti*-**1**, (c) *syn*-**1**.

The solid-state organization of *anti*-**1** exhibits characteristic ChB interactions found in organic selenocyanates. As shown in Figure 2, selenium atom Se1 acts as a twofold ChB donor, through its two sigma-holes, with one very short interaction (RR = 0.86), in the prolongation of the NC−Se(1) bond, toward N2A(−x, −y, −z), and one longer contact (RR = 0.93), in the prolongation of the CH_2−Se(1) bond, toward N1(−0.5+x, 0.5−y, z). On the other hand, selenium atom Se2 in not engaged at all in such a Se•••N ChB but makes an inversion-centered Se(2A)•••Se(2A) motif (3.391(6) Å, RR = 0.89) analogous to the so-called type I halogen-bonded motifs found in halogenated molecules. This complex behavior contrasts with that found for the less-substituted achiral derivatives such as the bis(selenocyanato) o-, m-, p-xylylenes where •••NC−Se(R)•••NC−Se(R)••• chains are systematically observed. It probably comes as a consequence of the steric constraint brought by the two extra methyl substituents in *anti*-**1**. The situation is different in *syn*-**1**. As shown in Figure 3, each of the two selenium atoms acts here as ChB donor toward the nitrogen atom of the selenocyanate of neighboring molecules, giving the recurrent chains mentioned above, with however larger intermolecular distances (RR = 0.89, 0.95) and poorer directionality (the NC−Se••N angles here are only 162 and 127° only).

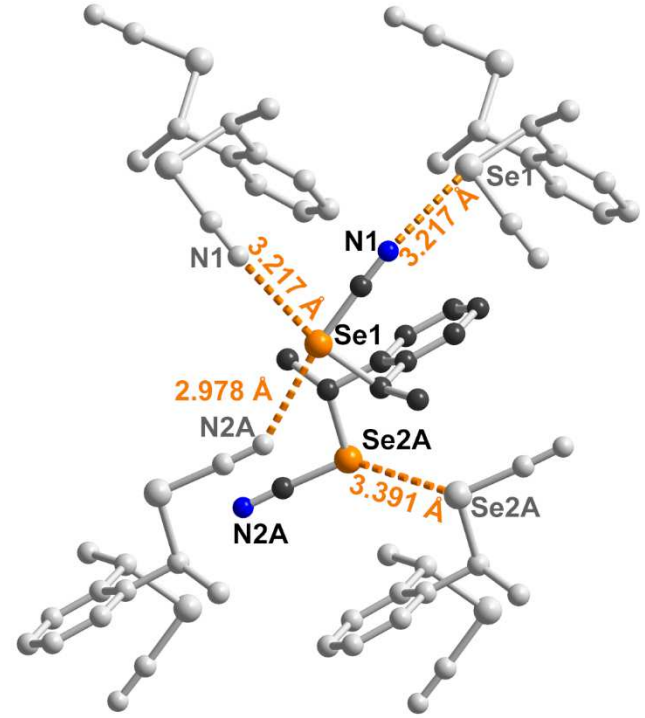

Fig. 2 Details of the ChB interactions in *anti*-**1**. Only the major component of the disordered SeCN group is shown. Relevant bond distances and angles: Se(1)•••N(2A)^{i} 2.978(25) Å, C(9-)–Se(1)•••N(2)^{i}: 172.7(5)°; Se(1)–N(1)^{ii} 3.217(3) Å, C(7)–Se(1)•••N(1)^{ii} 167.9(8)° (i : –x, –y, –z ; ii : –0.5+x, 0.5–y, z).

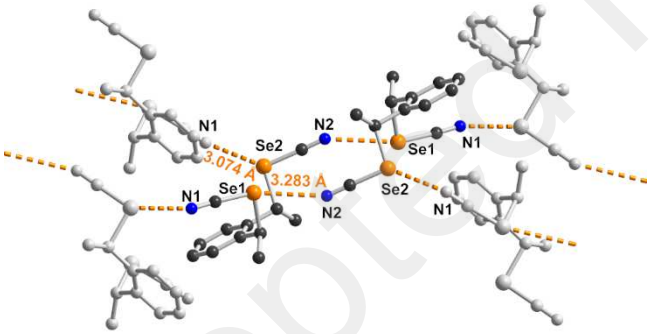

Fig. 3 Details of the ChB interactions in *syn*-**1**. Relevant bond distances and angles: Se(1)•••N(2)^{i} 3.283(7) Å, C(9)–Se(1)•••N(2)^{i}: 162.6(2)°; Se(2)•••N(1)^{ii} 3.074(7) Å, C(12)–Se(2)–N(1) 127.05(25)° (i : 1–x, –1–y, 1–z ; ii : 1–x, –0.5+y, 0.5–z).

Co-crystal formation with *anti*-**1** was investigated with both neutral Lewis bases such as 4,4'-bipyridine and anionic halide salts such as Ph_4PX (X = Cl^-, Br^-, I^-). With 4,4'-bipyridine, co-crystallization afforded a chalcogen-bonded structure of 2:1 stoichiometry formulated as (*anti*-**1**)$_2$(bipy). It crystallizes in the monoclinic system, S.G. $P2_1/a$ with the 4,4'-bipyridine on inversion center, linking the inversion-related enantiomers of *anti*-**1** (Figure 4). Both selenium atoms act here as ChB donors toward the pyridinic nitrogen atom, with one very short ChB, for Se(1)•••N(3) (RR = 0.87) while the Se(2)•••N(3) interaction is essentially at van

der Waals contact distance, with a marked directionality for both interactions as the NC–Se•••N(3) angle amounts to 173.62(13) and 168.66(11)° respectively. Besides, the Se2 selenium atom acts as ChB donor through its second, weaker σ-hole located in the prolongation of the CH_2–Se bond in a Se(2)•••N2 contact while Se(1) forms an inversion-centered , Type I, Se•••Se motif. Note that the co-crystals formed from 4,4'-bipyridine and the unsubstituted *meta*- or *para*- bis(selenocyanato)xylylenes are characterized with notably stronger Se•••N ChB interactions with RR values in the range 0.82-0.84.[24a]

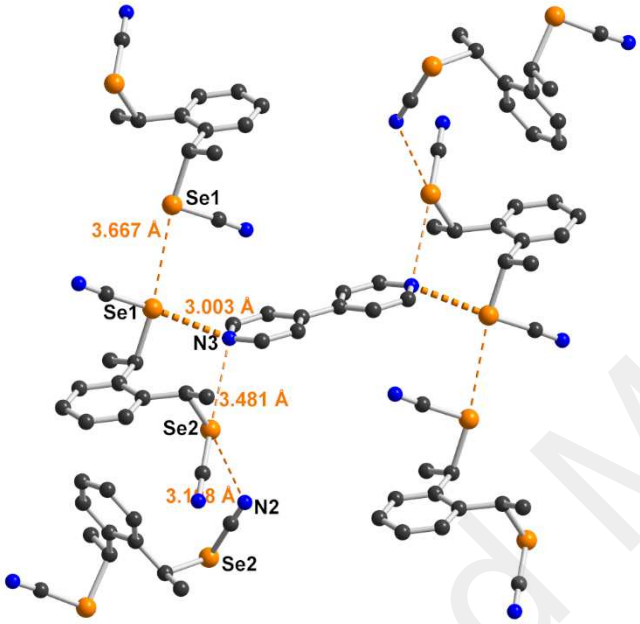

Fig. 4 Detail of the trimolecular adduct between *anti*-**1** and 4,4'-bipyridine. The strongest interaction is highlighted with a thicker dotted line. Relevant bond distances and angles: Se(1)•••N(3): 3.003(4) Å, C(9)–Se(1)•••N(3) 173.62(13)°; Se(2)•••N(3) 3.481(3) Å, C(12)–Se(2)•••N(3) 168.66(11)°; Se(2)•••N(2)^{i} 3.198(3) Å, C(11)•••Se(2)•••N(2)^{i} 141.06(8)°; Se(1)•••Se(1)^{ii} 3.667(1) (i: 0.5+x, 0.5–y, z ; ii: –x, –y, 2–z).

Co-crystals of *anti*-**1** with the three tetraphenyl phosphonium halides, i.e. Ph_4PCl, Ph_4PBr and Ph_4PI, all crystallize in a 1:1 stoichiometry with the halide in a μ_2 environment, chelated by the ditopic ChB donor. The chloride and bromide salts are isostructural, and crystallize as Et_2O solvate in the triclinic system, S. G. $P\bar{1}$, with the anionic complex in general position. As shown in Figures 5a-5b, the environment of the Cl^- and Br^- anions is distorted with one (NC)–Se•••X^- ChB slightly shorter than the other. In both cases, the overall Se•••X^- distance corresponds to a reduction ratio (considering the ionic radius of the halide rather than its van der Waal radius, i.e. Cl^-: 1.81 Å, Br^-: 1.96 Å, I^-: 2.20 Å) in the range 0.88–0.90. These

values are notably larger than those reported earlier in the unsubstituted achiral analogs chelating Cl^- or Br^- anions which exhibit RR values as small as 0.84.[25]

The situation is more complex in the iodide adduct (Figure 5c). It crystallizes without solvent in the orthorhombic system, space group $P2_12_12_1$, with the anionic complex in general position. The Se•••I^- distances are here associated with RR values of 0.88-0.89 and one (N)C–Se••I– angle deviates notably from 180° (167°).

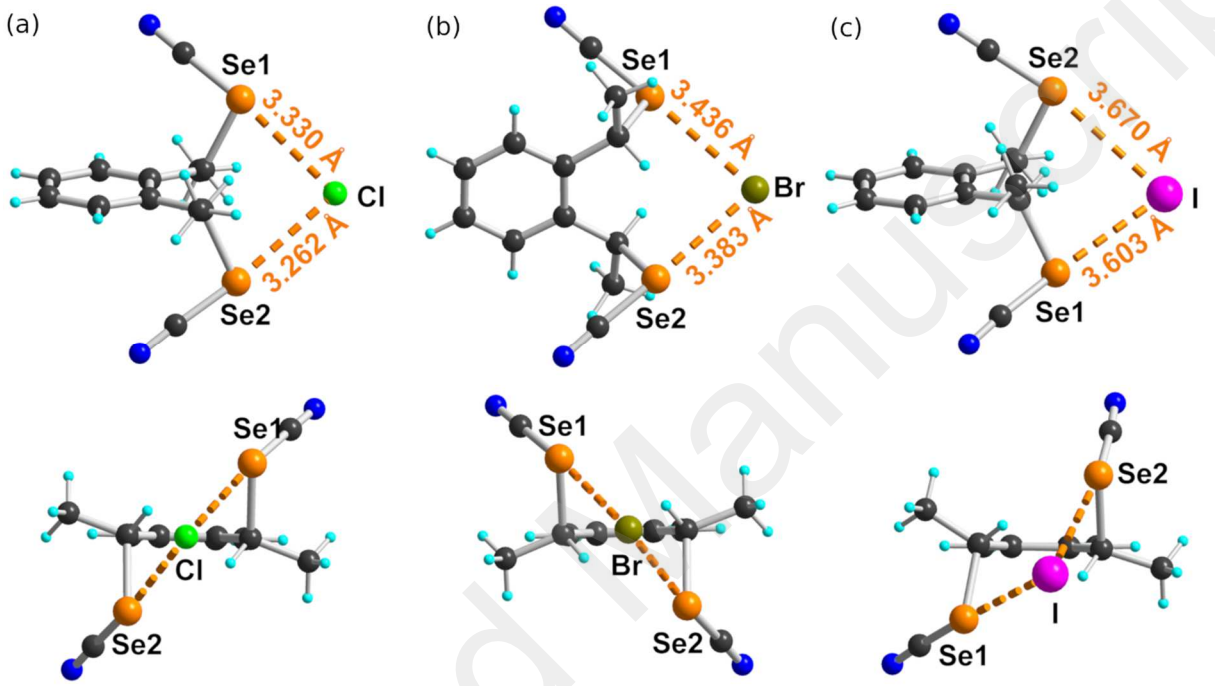

Fig. 5 Detail of the three halide adducts with structural characteristics in: (a) Ph_4P^+[(*anti*-**1**)Cl^-]•$(Et_2O)_{0.5}$, (b) Ph_4P^+[(*anti*-**1**)Br^-]•$(Et_2O)_{0.5}$,and (c) Ph_4P^+[(*anti*-**1**)I^-]. Relevant bond distances and angles: Se(1)•••Cl: 3.330(7) Å, (N)C–Se(1)•••Cl: 173.75(13)°, Se(2)•••Cl: 3.262(6) Å, (N)C–Se2•••Cl: 173.67(13)°; Se(1)•••Br 3.436(4) Å, (N)C–Se(1)•••Br: 175.12(13)°, Se(2)•••Br: 3.383(3) Å, (N)C–Se2•••Br: 174.48(13)°; Se(1)•••I: 3.603(1) Å, (N)C–Se(1)•••I: 177.6(2)°, Se(2)•••I: 3.670(1) Å, (N)C–Se(2)•••I: 167.8(2)°.

These three structures and the relatively long Se•••X^- distances seem to indicate that the introduction of the methyl substituents on the benzylic positions induces, in the *anti*-isomer at least, an unfavorable effect on the ChB donor ability of this chelating system. At first sight, this effect might have two origins, (i) the electron-donating effect of the methyl groups might decrease the overall ChB donor ability of the selenium atoms, and/or (ii) the steric constraints brought by the methyl groups do not favor the optimal "coordination" of the halide anion, at least in the *anti* conformation of the chelate.

One first element of answer can be already found in the crystal structure obtained from the association of Et_4NCl and the *syn* isomer, using a *syn*-enriched sample. A 2:1 association

formulated as (Et_4N^+)[(*syn*-**1**)$_2Cl^-$] is indeed isolated, which crystallizes in the monoclinic system, S. G. $P2_1/a$, with the Cl^- anion on inversion center in a μ_4, square-planar environment (Figure 6). The Se•••Cl^- distances are very short (3.11, 3.16 Å, RR = 0.84-0.85), and furthermore even shorter than those reported in the chloride adduct of the achiral chelating *ortho*-bis(selenocyanate)xylylene A (3.17–3.20 Å, RR = 0.85-0.86) or the 1,2,4,5-tetrakis(selenocyanoatomethyl)benzene E (3.16–3.22 Å, RR = 0.85-0.87).[25]

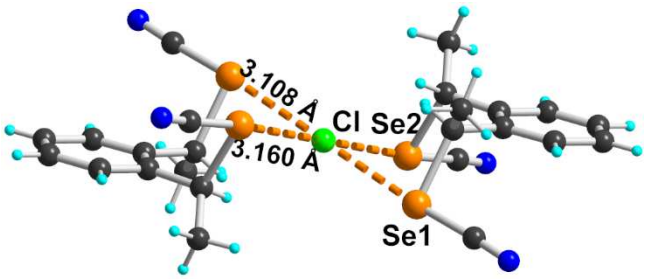

Fig. 6 Detail of the anionic moiety [(*syn*-**1**)$_2Cl^-$] in its Et_4N^+ salt. Relevant bond distances and angles: Se(1)•••Cl: 3.108(3) Å, C–Se(1)•••Cl: 176.2(2)°; Se(2)•••Cl: 3.160(1) Å, C–Se(2)•••Cl: 176.0(3)°.

In order to rationalize these differences, theoretical calculations of the relative energies of the molecules (*anti vs. syn*) and their Cl^- adducts were performed. Total energy for the *syn* and *anti* forms of **1** was calculated [B3LYP 6-311++G(d,p)] after geometry optimization, keeping the C_2 geometry of the *anti* form, and the C_s geometry of the *syn* form (Figure 7). Under these conditions, the *anti* form is more stable by 2.31 kcal/mol (9.7 kJ/mol) than the *syn* form. Without symmetry constraints, the *syn* form is able to stabilize through an intramolecular Se•••Se ChB interaction (3.958 Å) reducing the difference to 0.68 kcal/mol (2.8 kJ/mol).

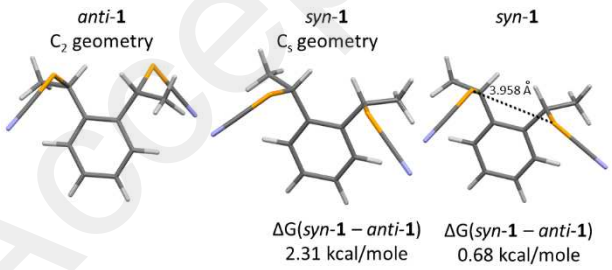

Fig. 7 Optimized geometries of *anti*-**1** and *syn*-**1** with and without symmetry constraints.

The evolution of the σ-hole amplitude has been determined for three molecules bearing, either a methyl group on each benzylic carbon (that is in *anti*-**1** and *syn*-**1**), or a hydrogen atom (that is the unsubstituted molecule A in scheme 1), or, for comparison purposes, a fluorine atom

(instead of a methyl group) in the fluorine-substituted derivatives of A, that is *anti*-**3** and *syn*-**3**. As shown in Figure 8a, we note a very small difference between *anti*-**1** and *syn*-**1**, with $V_{s,max}$ values of 46.26 and 47.05 kcal/mol respectively, i.e. a slightly larger $V_{s,max}$ value for *syn*-**1**. Such a small difference cannot explain the much shorter ChB interaction experienced with the Cl^- anion with *syn*-**1** (See above). The evolution in the series of substituents $Me_2/H_2/F_2$ follows the expected trend, with a strengthening of the $V_{s,max}$ in the order $F_2 > H_2 > Me_2$ associated with the electron withdrawing effect of the fluorine atoms. Furthermore, an even stronger electropositive area (54.3 kcal mol^{-1}) is identified in the fluorine substituted *syn*-**3** in-between the two activated benzylic hydrogen atoms located α to the fluorine atoms. These calculations demonstrate that, whatever the substituents, the *syn* form exhibits systematically a slightly stronger σ-hole than the *anti* form. However, they are unable to explain the much shorter ChB interaction with Cl^-.

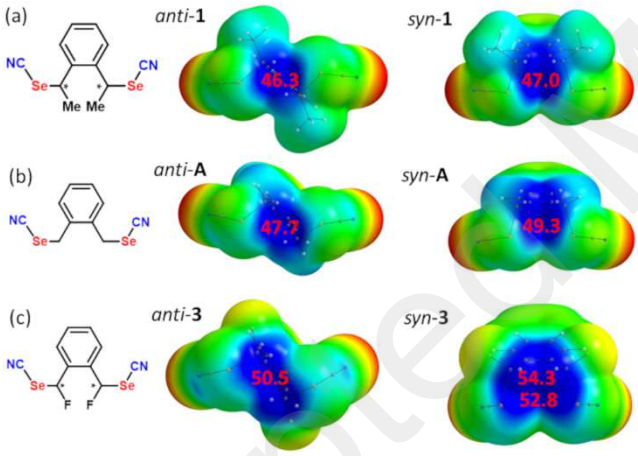

Fig. 8 Details of the ESP maps of (a) methyl-substituted *anti*-**1** and *syn*-**1**, (b) unsubstituted A and (c) fluorine-substituted *anti*-**3** and *syn*-**3**, at optimized geometries, plotted on the 0.001 electron/$bohr^3$ isosurface of the electronic density. The extrema values $V_{s,max}$ (kcal/mol) of the electropositive (blue) area are indicated in red numbers. Potential scale ranges from –25.1 kcal/mol (red) to +37.7 kcal/mol.

Calculations performed on 1:1 adducts between the *syn* and *anti* forms of **1** and a chloride anion give geometries very close to those observed in the crystal structures of $Ph_4P^+[(anti\text{-}\mathbf{1})Cl^-]\bullet(Et_2O)_{0.5}$ and $Et_4N^+[(syn\text{-}\mathbf{1})_2Cl^-]$ (Figure 9). The notably shorter Se•••Cl^- distances with *syn*-**1** (3.11-3.16 Å, *vs*. 3.26-3.33 Å with *anti*-**1**) is very well reproduced by the calculations which give a Se•••Cl^- distance at 3.139 Å in *syn*-**1**•Cl^- adduct (C_s geometry), notably smaller

indeed than the 3.210 Å distance calculated in *anti*-**1**•Cl^- adduct (C_2 geometry). The overall energy of both adducts is almost the same with ΔG(*syn*-**1**•Cl^- – *anti*-**1**•Cl^-) = 1.29 kcal/mole, that is a slightly more stable adduct with *anti*-**1**. On the other hand, the BSSE complexation energy (–35.36 kcal/mole for *anti*-**1**•Cl^-, –35.55 kcal/mol for *syn*-**1**•Cl^-) gives a small advantage to the *syn* adduct. It appears therefore that the shorter Se•••Cl^- ChB interaction experienced with the *syn*–**1** ChB donor is not associated with a sizeable stabilization of this chloride adduct, when compared with its *anti* analog. As shown in Figure 8, the electropositive area (in blue) interacting with Cl^- exceeds that delineated with the selenium atoms only and include also the two benzylic hydrogen atoms. The overall interactions in both adducts thus implies also C_{Bz}–H•••Cl^- contacts, whose geometrical features (for both experimental and calculated structures) are collected in Table 1. These contacts are quite short (2.79-2.86 Å for a contact distance of 3.01) Å even if they deviate notably from linearity (C–H•••Cl^- angles in the range 123-128°). Their contribution to the overall stabilization of the adducts can probably not be omitted.

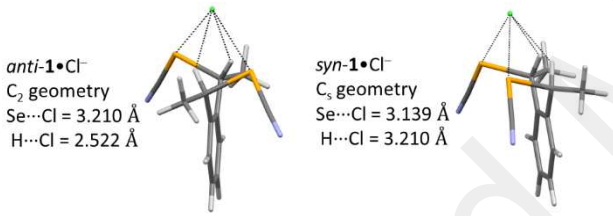

Fig. 9 Optimized geometries of the *anti*-**1**•Cl^- and *syn*-**1**•Cl^- adducts with indicated symmetry constraints.

Table 1 Structural characteristics of C–H•••Cl^- contacts, from X-ray crystal structures of Ph_4P^+[(*anti*-**1**)Cl^-]•$(Et_2O)_{0.5}$ and Et_4N^+[(*syn*-**1**)$_2Cl^-$] and from theoretical calculations on 1:1 adducts (in italics).

		H•••Cl^- dist (Å)	C–H•••Cl– ang. (°)
(*anti*-**1**)Cl^-	X-ray	2.863(6)	128.1(2)
		2.800(4)	127.0(2)
	calcd.	*2.522*	*138.1*
(*syn*-**1**)Cl^-	X-ray	2.794(2)	125.2(3)
		2.811(2)	123.0(4)
	calcd.	*2.573*	*134.9*

Conclusions

Introduction of methyl substituents on the achiral 1,2-bis(selenocyanatomethyl)benzene (A) leads to diastereoisomers of a novel chelating, chiral ChB donor, namely 1,2-bis(1-selenocyanatoethyl)benzene (**1**), as a mixture of the two *anti* enantiomers and the *syn* (*meso*) form. The *anti* (racemic) mixture was isolated in a pure form by recrystallization. We were able to isolate crystals of both *anti*-**1** and *syn*-**1**. Structure determinations show the recurrent formation of short Se•••N≡C ChB interactions (RR = 0.88-0.95). Co-crystallization of *anti*-**1** with 4,4'-bipyridine affords a 2:1 adduct, i.e. (*anti*-**1**)$_2$(bipy), with one very short Se•••N_{Py} ChB at 3.003 Å (RR = 0.87). Co-crystallization of *anti*-**1** with tetraphenylphosphonium halides (Cl^-, Br^-, I^-) provides the 1:1 adducts while a 2:1 adduct is isolated between *syn*-**1** and Et_4NCl, formulated as $Et_4N^+[(syn\text{-}\mathbf{1})_2Cl^-]$. Comparison of chloride chelation with *anti*-**1** and *syn*-**1** shows much shorter (NC)Se•••Cl^- ChB interactions with the *syn* isomer. Calculations of (i) the electrostatic surface potential of neutral ChB donors for σ-hole amplitude determination and (ii) the Cl^- BSSE complexation energy cannot explain these differences even if the geometry optimizations well reproduce them. Besides, the concomitant contribution of C–H•••Cl^- hydrogen bonds involving benzylic hydrogen atoms α to the SeCN moieties is highlighted. Altogether, the notably shorter Se•••Cl^- distances found with the *syn* isomer appear to be a mere consequence of the overall relative orientation of both selenocyanate moieties together with contribution of C_{Bz}–H•••Cl^- hydrogen bonds, as illustrated by the broader spatial expansion of the electropositive area observed in the *syn* isomer. This modulation of the ChB donor ability, combined with the introduction of chirality, provides novel chelating ChB donors which will be of interest in crystal engineering, anion recognition processes and catalysis. We are pursuing our works along these lines.

Experimental section

General remarks

NMR spectra were recorded at room temperature using $CDCl_3$ unless otherwise noted. Chemical shifts are reported in ppm and ^{1}H NMR spectra were referenced to residual $CHCl_3$ (7.26 ppm) and ^{13}C NMR spectra were referenced to $CHCl_3$ (77.2 ppm). All reagents are commercially available and were used without further purification. Melting points were measured on a Kofler hot-stage apparatus and are uncorrected. Elemental analysis were performed at BioCIS laboratory, UMR-8076-CNRS-University Paris-Saclay. All the reactions

were performed under an argon atmosphere. Methanol, acetonitrile and dichloromethane were dried using inert pure solvent column device.

Syntheses

1,2-bis(1-bromoethyl)benzene 2. In a 100 mL two-neck round-bottom flask equipped with condenser, 1,2-diethylbenzene (2 g, 14.9 mmol) and NBS (5.3 g, 29 mmol, 2 eq.) are dissolved in CCl_4 (30 mL) and warmed to reflux. After addition of a little AIBN, stirring is maintained for 30 minutes. Another small quantity of AIBN is added again. After an hour of stirring and cooling, the succinimide is eliminated by filtration. The filtrate is evaporated and the solid residue filtered through a silica column with petroleum ether as eluant. Evaporation of the solvent yields **2** as a white solid (2.93 g, 67%), in a ratio *anti*/*syn* of 70:30 (based on ^{1}H NMR). Pure *anti*-**2** is obtained by recrystallization in hexane, while the mother liquors are enriched in *syn* isomer in a ratio *anti*/*syn* of 23:77.

anti-**2** m. p. 89°C. ^{1} H NMR (300 MHz, $CDCl_3$) δ 2.15 (6H, d, J^3 = 6.84 Hz); 5.71 (2H, q, J^3 = 6.84); 7.34-7.40 (2H, m); 7.58-7.63 (2H, m)

syn-**2** ^{1} H NMR (300 MHz, $CDCl_3$) δ 2.10 (6H, d, J^3 =6.90 Hz); 5.61 (2H, q, J^3 = 6.90); 7.32-7.38 (2H, m); 7.58-7.63 (2H, m).

1,2-bis(1-selenocyanatoethyl)benzene 1. To a solution of *anti*-**2** (0.59 g, 2 mmol) dissolved in acetone (5 mL) at room temperature, KSeCN (0.87g, 6 mmol, 3 eq.) dissolved in warm acetone (5 mL) is added dropwise over a period of 10 minutes. After 30 minutes of stirring, the suspension is filtered, the filtrate is evaporated, and the resulting solid dissolved in CH_2Cl_2 (10 mL) and washed with water (2 × 10 mL). The organic layers are collected, dried with $MgSO_4$, filtered and evaporated to give **1** (0.59 g, 86%) as a white solid in a ratio *anti*/*syn* of 76:24 (based on NMR). Pure sample of *anti*-**1** is obtained from recrystallization in acetone. The same reaction performed with **2** in a *anti*/*syn* ratio of 23:77 afforded **1** in a *anti*/*syn* ratio of 66:34.

anti-**1**: M. p. 113°C; ^{1} H NMR (300 MHz, $CDCl_3$) δ 2.12 (6H, d, J^3 = 6.9 Hz); 5.25 (2H, q, J^3 = 6.9); 7.40-7.45 (2H, m); 7.54-7.59 (2H, m). ^{13}C NMR: 22.58 (CH_3); 40.00 (<u>C</u>H-CH_3); 101.86; 127.24; 129.65, 137.06. Elem. Anal. Calcd. for $C_{12}H_{12}N_2Se_2$: C, 42.12; H, 3.54; N, 8.19; found: C, 41.92; H, 3.57; N, 8.20. Mother liquors are enriched in *syn* compound with a *syn:anti* distribution of 67:33. Their dissolution in acetone and diffusion of hexane afforded a few crystals of *syn*-**1** suitable for X-ray diffraction. *syn*-**1**: ^{1} H NMR (300 MHz, $CDCl_3$) δ 2.15 (6H,

d, J^3 = 6.90 Hz); 5.17 (2H, q, J^3 = 6.90); 7.40-7.45 (2H, m); 7.54-7.59 (2H, m). ^{13}C NMR: 24.03 (CH_3); 40.11 ($\underline{C}H$-CH_3); 101.97; 127.58; 129.69, 136.84.

(*anti*-1)$_2$(4,4'-bipy). In a small test tube, 4,4'-bipyridine (10 mg, 0.06 mmol) and *anti*-**1** (11 mg, 0.03 mmol) are dissolved in acetone (1 mL). Diffusion of Et_2O vapors affords after 5 days colorless crystals of (*anti*-**1**)$_2$(4,4'-bipy). Elem. Anal. Calcd. for $C_{34}H_{32}N_6Se_4$: C, 48.59; H, 3.84; N, 10.00; found: C, 48.57; H, 3.91; N, 9.95.

Ph_4PCl(*anti*-1)•(Et_2O)$_{0.5}$ In a small tube, *anti*-**1** (11 mg, 0.03 mmol) and Ph_4PCl (13.5 mg, 0.036 mmol,) were dissolved in acetonitrile (1 mL). The tube was placed into a small bottle with ether for diffusion crystallization. Crystals were isolated after 5 days. Exact composition was deduced from X-ray diffraction. Elem. Anal. Calc. for $C_{36}H_{32}ClN_2PSe_2$ (without Et_2O): C, 60.3; H, 4.5; N, 3.91; found: C, 56.21; H, 4.62; N, 4.20.

Ph_4PBr(*anti*-1)•(Et_2O)$_{0.5}$ In a small tube, *anti*-**1** (10 mg, 0.03 mmol) and Ph_4PBr (17.7 mg, 0.042 mmol) were dissolved in 1 mL of acetonitrile. The tube was placed into a small bottle with ether for diffusion crystallization. Crystals were isolated after 5 days. Exact composition was deduced from X-ray diffraction. Elem. Anal. Calcd. for $C_{36}H_{32}BrN_2PSe_2$ (without Et_2O): C, 56.78; H, 4.24; N, 3.68; found: C, 56.98; H, 4.71; N, 2.34.

Ph_4PI(*anti*-1). In a small tube, *anti*-**1** (13 mg, 0.04 mmol, 1 equiv) and Ph_4PI (21 mg, 0.045 mmol, 1 equiv) were dissolved in 1 mL of acetonitrile. The tube was put into a small bottle with ether for diffusion crystallization. Crystals were isolated after 5 days. Elem. Anal. Calcd. for $C_{36}H_{32}IN_2PSe_2$: C, 53.48; H, 3.99; N, 3.47; found: C, 54.43; H, 4.02; N, 3.42.

Et_4NCl(*syn*-1)$_2$. In a small tube, a 67/33 mixture of *syn*-**1**/*anti*-**1** (10 mg, 0.03 mmol) and Et_4NCl (4.9 mg, 0.03 mmol) were dissolved in acetone (1 mL). The tube was placed into a small closed bottle with hexane for diffusion crystallization. Crystals were isolated after 5 days. Elem. Anal. Calcd. for $C_{32}H_{44}ClN_5Se_4$: C, 45.22; H, 5.22; N, 8.24; found: C, 44.88; H, 6.13; N, 7.97.

Crystallography Details of the structural analyses for the eight compounds are summarized in Table 2. Single crystals were coated with Paratone-N oil and mounted on a MicroMount loop. The crystallographic data were collected at 296(2)K on a Bruker AXS APEX II diffractometer with Mo-Kα radiation (λ = 0.71073 Å) for all compounds except *anti*-**1** and *anti*-**2** which were collected on a Bruker AXS D8 Venture diffractometer equipped with a Mo-Kα microsource and a PHOTON 100 detector at 150(2) K. The structures were solved by dual-space algorithm using SHELXT programs[33] and then refined with full-matrix least-squares methods based on

F^2 (SHELXL-2014)[34] with the aid of the WinGX program.[35] All non-hydrogen atoms were refined with anisotropic atomic displacement parameters. Crystallographic data have been deposited with Cambridge Crystallographic Data Centre, CCDC: 2040289-2040296.

Table 2 Crystallographic data

Compound	*anti*-**1**	*syn*-**1**	*anti*-**2**	(*anti*-**1**)$_2$•bipy
Formula	$C_{12}H_{12}N_2Se_2$	$C_{12}H_{12}N_2Se_2$	$C_{10}H_{12}Br_2$	$C_{17}H_{16}N_3Se_2$
FW (g.mol^{-1})	342.16	342.16	292.02	420.25
Crystal system	monoclinic	monoclinic	monoclinic	monoclinic
Space group	$P2_1/a$	$P2_1/n$	$P2_1/n$	$P2_1/a$
a (Å)	7.5686(4)	8.5502(6)	8.2203(8)	7.1221(4)
b (Å)	21.7486(11)	7.0090(4)	14.6643(16)	28.6165(13)
c (Å)	8.2075(4)	22.6261(15)	9.4380(9)	8.6600(5)
α (°)	90.00	90.00	90.00	90.00
β (°)	105.783(2)	90.121(3)	110.312(3)	105.763(2)
γ (°)	90.00	90.00	90.00	90.00
V (Å^3)	1300.07(11)	1355.94(15)	1066.96(19)	1698.62(16)
T (K)	150(2)	296(2)	150(2)	296(2)
Cryst. dim. (Å^3)	0.16×0.12×0.05	0.23×0.17×0.02	0.12×0.09×0.02	0.26×0.21×0.18
Z	4	4	4	4
D_{calc} (g·cm^{-3})	1.748	1.676	1.818	1.643
μ (mm^{-1})	5.663	5.429	7.544	4.353
Abs. corr.	multi-scan	multi-scan	multi-scan	multi-scan
T_{min}, T_{max}	0.447, 0.753	0.344, 0.897	0.447, 0.860	0.347, 0.457
Total refls.	20013	22207	19035	12513
Uniq. refls. (R_{int})	2993 (0.0572)	3062 (0.0753)	2439 (0.0571)	3912 (0.0291)
Unique refls. (I>2s(I))	2631	1862	1943	3041
R_1	0.027	0.0495	0.0220	0.0367
wR_2 (all data)	0.066	0.1128	0.0513	0.0717
GoF	1.067	1.076	1.052	1.085
Res. dens (e$^-$ Å^{-3})	0.50, –0.65	0.41, –0.52	0.43, –0.78	0.39, –0.64

Table 2 (continued)

Compound	Ph_4PCl(*anti*-**1**) •0.5 Et_2O	Ph_4PBr(*anti*-**1**) •0.5 Et_2O	Ph_4PI(*anti*-**1**)	Et_4NCl(*syn*-**1**)$_2$
CCDC				
Formula	$C_{38}H_{37}ClN_2O_{0.50}PSe_2$	$C_{38}H_{37}BrN_2O_{0.50}PSe_2$	$C_{36}H_{32}IN_2PSe_2$	$C_{16}H_{22}Cl_{0.50}N_{2.50}Se_2$
FW (g.mol^{-1})	754.03	798.49	808.42	425
Crystal system	triclinic	triclinic	orthorhombic	monoclinic
Space group	$P\bar{1}$	$P\bar{1}$	$P2_12_12_1$	$P2_1/c$
a (Å)	9.2775(11)	9.3752(5)	9.2747(2)	9.0534(5)
b (Å)	13.5469(16)	13.5967(6)	10.6749(2)	13.1176(6)
c (Å)	14.3091(15)	14.3500(7)	34.3002(6)	16.4261(7)
α (°)	82.498(4)	82.051(2)	90.00	90.00
β (°)	88.218(4)	87.549(2)	90.00	112.672(2)
γ (°)	83.497(4)	83.173(2)	90.00	90.00
V (Å^3)	1771.3(4)	1798.15(15)	3395.94(11)	1800.00(15)
T (K)	296(2)	296(2)	296(2)	296(2)
Cryst. dim. (Å^3)	0.23×0.11×0.10	0.28×0.16×0.13	0.22×0.10×0.08	0.25×0.21×0.01
Z	2	2	4	4
D_{calc} (g·cm^{-3})	1.414	1.475	1.581	1.568
μ (mm^{-1})	2.238	3.242	3.161	4.179
Abs. corr.	multi-scan	multi-scan	multi-scan	multi-scan
T_{min}, T_{max}	0.744, 0.799	0.542, 0.656	0.691, 0.777	0.366, 0.959
Total refls.	43521	29306	24731	4122
Uniq. refls. (R_{int})	8141 (0.0375)	8249 (0.0298)	7781 (0.0247)	4121
Unique refls. (I>2s(I))	5829	5578	6512	2069
R_1	0.0434	0.0371	0.0327	0.0624
wR_2 (all data)	0.1222	0.091	0.070	0.1591
GoF	1.142	1.059	1.02	1.027
Res. dens (e$^-$ Å^{-3})	0.652, –0.951	0.898, –-0.596	0.557, –0.391	0.568, –0.561
Flack param.	–	–	0.64(1)	–

Theoretical calculations

Theoretical calculations were performed using the Gaussian09 software[36] at the DFT level employing the B3LYP functional and the 6-311++G(d,p) basis set. Molecular structures of *anti*-**1**, *syn*-**1**, *anti*-**A**, *syn*-**A**, fluorine-substituted *anti*-**3** and *syn*-**3** were optimized and frequency calculations were performed in order to check that true energy minima were obtained. Electrostatic potential (ESP) mapped on the ρ = 0.001 a.u. isodensity surface were then computed with the AIMAll software package;[37] the maximum of ESP $V_{S,max}$ in the region of the (NC)Se σ-holes associated with Se atoms were located with MultiWFN software.[38]

Whereas *anti*-**1** optimized under C2 symmetry toward a true energy minimum, *syn*-**1** optimized toward a Cs molecular structure associated with a small imaginary frequency (−20 cm^{-1}). Further optimization of that structure without symmetry constrain led to a true energy minimum characterized by an intramolecular Se•••Se interaction [d(Se•••Se) = 3.958 Å, RR = 1.04; α(C−Se•••Se) = 154.6°)], with the (NC)Se σ-hole of one of the two selenium atoms pointing toward one lone pair of the second chalcogen atom. The Cs constrained *syn*-**1** molecular structure is then reported for comparison purposes, since in that structure the two chalcogen (NC)Se σ-holes are oriented as in the halide adducts. The same situation occurs for *syn*-**A** which was calculated under constrained Cs symmetry (imaginary frequency = −12 cm^{-1}; the two σ-holes pointing outward the molecule) and also under C1 [intramolecular Se•••Se interaction d(Se•••Se) = 3.692 Å, RR = 0.97; α(C−Se•••Se) = 169.4°]. For fluorine-substituted *syn*-**3** molecule, the Cs symmetry constrained structure is also a saddle point (imaginary frequency = −9 cm^{-1}; the two σ-holes pointing outward the molecule) but the unconstrained C1 symmetry structure does not present the previously observed intramolecular Se•••Se interaction due to an unfavorable relative NCSe orientations [d(Se•••Se) = 4.044 Å, RR = 1.06; α(C−Se•••Se) = 128.4°].

Molecular structures of the (*anti*-**1**)Cl^- and (*syn*-**1**)Cl^- were also optimized using the same calculation conditions and true energy minima were obtained. Basis Set Superposition Error corrected structures and complexation energies were obtained through the counterpoise method of Boys & Bernard.[39] More details are given in the Supporting Information file (cartesian coordinates of optimized molecular structures).

Conflicts of interest

There are no conflicts to declare.

Acknowledgements

This work was supported by the French National Agency for Research (ANR 17-CE07-0025-01 and ANR 17-CE07-0025-02. The EXPLOR mesocentre is thanked for computing facilities (Project 2019CPMXX0984).

References

[1] (*a*) J.-M. Lehn, *Chem. Soc. Rev*., 2007, **36**, 151−160. (*b*) Y. Zhao, Y. Cotelle, N. Sakai and S. Matile, *J. Am. Chem. Soc*., 2016, **138**, 4270−4277.

[2] (a) G. Cavallo, P. Metrangolo, R. Milani, T. Pilati, A. Priimagi, G. Resnati and G. Terraneo, *Chem. Rev*., 2016, **116**, 2478–2601. (*b*) L. C. Gilday, S. W. Robinson, T. A. Barendt, M. J. Langton, B. R. Mullaney and P. D. Beer, *Chem. Rev*., 2015, **115**, 7118–7195.

[3] T. Clark, M. Hennemann, J. S. Murray and P. Politzer, *J. Mol. Mod*., 2007, **13**, 291−296.

[4] (*a*) A. Bauza, T. J. Mooibroek and A. Frontera, *Angew chem. Int. Ed*., 2013, **52**, 12317−12321. (*b*) A. Bauza, S. K. Seth and A. Frontera, *Coord. Chem. Rev*., 2019, **384**, 107−125.

[5] (*a*) L. M. Lee, M. Tsemperoli, A. I. Poblador-Bahamonte, S. Benz, N. Sakai, K. Sugihara and S. Matile, *J. Am. Chem. Soc*., 2019, **141**, 810−814. (*b*) P. Scilabra, G. Terraneo and G. Resnati, *J. Fluor. Chem*., 2017, **203**, 62−74.

[6] (*a*) P. Scilabra, G. Terraneo and G. Resnati, *Acc. Chem. Res*., 2019, **52**, 1313−1324. (*b*) K. T. Mahmudov, M. N. Kopylovich, M. F. C. Guedes da Silva and A. J. L. Pombeiro, *Dalton Trans*., 2017, **46**, 10121−10138. (*c*) L. Vogel, P. Wonner and S. M. Huber, *Angew. Chem. Int. Ed.*, 2019, **58**, 1880 –1891. (*d*) N. Biot and D. Bonifazi, *Coord. Chem. Rev*., 2020, **413**, 213243. (e) C. B. Aakeroy, D. L. Bryce, G. R. Desiraju, A. Frontera, A. C. Legon, F. Nicotra, K. Rissanen, S. Scheiner, G. Terraneo, P. Metrangolo and G. Resnati, *Pure Appl. Chem*., 2019, **91**, 1889–1892.

[7] N. Biot and D. Bonifazi, *Chem. Eur. J*., 2020, **26**, 2904 – 2913.

[8] (*a*) P. Wonner, L. Vogel, M. Düser, L. Gomes, F. Kniep, B. Mallick, D. B. Werz and S. M. Huber, *Angew. Chem. Int. Ed*., 2017, *56*, 12009−12012. (b) P. Wonner, L. Vogel, F. Kniep and S. M. Huber, *Chem. Eur. J*., 2017, **23**,16972–16975. (*c*) S. Benz, J. Mareda, C. Besnard, N. Sakai and S. Matile, *Chem. Sci*., 2017, **8**, 8164 –8169. (*d*) S. E. Reisman, A. G. Doyle and E. N. Jacobsen, *J. Am. Chem. Soc*., 2008, **130**, 7198–7199. (e) W. Wang, H. Zhu, S. Liu, Z. Zhao, L. Zhang, J. Hao and Y. Wang, *J. Am. Chem. Soc*., 2019, **141**, 9175−9179.

[9] (*a*) M. S. Taylor, *Coord. Chem. Rev*., 2020, **213**, 213270. (*b*) E. Navarro-Garcia, B. Galmés, M. D. Velasco, A. Frontera and A. Caballero, *Chem. Eur. J*., 2020, **26**, 4706–4713. (*c*) J. Y. C. Lim, J. Y. Liew and P. D. Beer, *Chem. Eur. J*., 2018, **24**, 14560–14566.

[10] S. Benz, M. Macchione, Q. Verolet, J. Mareda, N. Sakai and S. Matile, *J. Am. Chem. Soc*., 2016, **138**, 9093–9096.

[11] M. Macchione, A. Goujon, K. Strakova, H. V. Humeniuk, G. Licari, E. Tajkhorshid, N. Sakai and S. Matile, *Angew. Chem. Int. Ed*., 2019, **58**, 15752–15756.

[12] (*a*) M. E. Brezgunova, J. Lieffrig, E. Aubert, S. Dahaoui, P. Fertey, S. Lebègue, J. G. Angyan, M. Fourmigué and E. Espinosa, *Cryst. Growth. Des*., 2013, **13**, 3283–3296. (*b*) H. Wang, J. Liu and W. Z. Wang, *Phys. Chem. Chem. Phys*., 2018, **20**, 5227–5234.

[13] P. Politzer, J. S. Murray, T. Clark and G. Resnati, *Phys. Chem. Chem. Phys.,* 2017, **19**, 32166–32178.

[14] P. C. Ho, P. Szydlowski, J. Sinclair, P. J.W. Elder, J. Kübel, C. Gendy, L. M. Lee, H. Jenkins, J. F. Britten, D. R. Morim and I. Vargas-Baca, *Nature Commun*., 2016, **7**, 11299.

[15] G. E. Garrett, E. I. Carrera, D. S. Seferos and M. S. Taylor, *Chem. Commun*., 2016, **52**, 9881–9884.

[16] M. Macchione, M. Tsemperouli, A. Goujon, A. R. Mallia, N. Sakai, K. Sugihara and S. Matile, *Helv. Chim. Acta*., 2018, **101**, e1800014.

[17] N. Biot and D. Bonifazi, *Chem. Eur. J*., 2018, **24**, 5439–5443.

[18] (*a*) A. F. Cozzolino, I. Vargas-Baca, S. Mansour and A. H. Mahmoudkhani, *J. Am. Chem. Soc*., 2005, **127**, 3184–3190 (*b*) V. Kumar, Y. Xu and D. L. Bryce, *Chem. Eur. J*., 2020, **26**, 3275–3286. (*c*) G. E. Garrett, G. L. Gibson, R. N. Straus, D. S. Seferos and M. S. Taylor, *J. Am. Chem. Soc*., 2015, **137**, 4126–4133.

[19] J. Y. C. Lim, I. Marques, A. L. Thompson, K. E. Christensen, V. Felix and P. D. Beer, *J. Am. Chem. Soc*., 2017, **139**, 3122–3133.

[20] A. Dhaka, O. Jeannin, I.-R. Jeon, E. Aubert, E. Espinosa and M. Fourmigué, *Angew. Chem. Int. Ed*., 2020, in press, DOI 10.1002/anie.202011981

[21] M. Beau, S. Lee, S. Kim, W.-S. Han, O. Jeannin, M. Fourmigué, E. Aubert, E. Espinosa, and I.-R. Jeon, *Angew. Chem. Int. Ed*., 2020, in press, DOI 10.1002/anie.202010462

[22] J. George, V. L. Deringer and R. Dronskowski, *J. Phys. Chem. A*., 2014, **118**, 17, 3193–3200.

[23] O. Jeannin, H.-T. Huynh, A. M. S. Riel and M. Fourmigué, *New J. Chem*., 2018, **42**, 10502–10509.

[24] (*a*) H.-T. Huynh, O. Jeannin and M. Fourmigué, *Chem. Commun*., 2017, **53**, 8467–8469. (*b*) A. M. S. Riel, O. Jeannin, O. B. Berryman and M. Fourmigué, *Acta Cryst.* 2019, **B75**, 34–38.

[25] A. M. S. Riel, H.-T. Huynh, O. Jeannin, O. Berryman and M. Fourmigué, *Cryst. Growth Des*., 2019, **19**, 1418–1425.

[26] V. Kumar, C. Leroy and D. L. Bryce, *CrystEngComm*, 2018, **20**, 6406–6411.

[27] R. Weiss, E. Aubert, P. Peluso, S. Cossu, P. Pale and V. Mamane, *Molecules* 2019, **24**, 4484 (1-16).

[28] (*a*) K. Fujita, M. Iwaoka and S. Tomoda, *Chem. Lett*., 1994, **23**, 923–926. (*b*) T. Wirth, *Angew. Chem. Int. Ed*., 1995, **34**, 1726–1728.

[29] V. Mamane, P. Peluso, E. Aubert, R. Weiss, E. Wenger, S. Cossu and P. Pale, *Organometallics*, 2020, in press, DOI 10.1021/acs.organomet.0c00633.

[30] S. M. Walter, F. Kniep, E. Herdtweck and S. M Huber, *Angew. Chem. Int. Ed*., 2011, **50**, 7187–7191.

[31] E. Eru, G. E. Hawkes, J. H. P. Utley and P. B. Wyatt, *Tetrahedron*, 1995, **51**, 3033–3044.

[32] D.-R. Hou, M.-S. Wang, M.-W. Chung, Y.-D. Hsieh and H.-H. G. Tsai, *J. Org. Chem*., 2007, **72**, 9231–9239.

[33] G. M. Sheldrick, Acta Cryst., 2015, **A71**, 3–8.

[34] G. M. Sheldrick, Acta Cryst., 2015, **C71**, 3–8.

[35] J. Farrugia, *J. Appl. Crystallogr*., 2012, **45**, 849–854.

[36] M. J. Frisch, G. W. Trucks, H. B. Schlegel, G. E. Scuseria, M. A. Robb, J. R. Cheeseman, G. Scalmani, V. Barone, B. Mennucci, G. A. Petersson, H. Nakatsuji, M. Caricato, X. Li, H. P. Hratchian, A. F. Izmaylov, J. Bloino, G. Zheng, J. L. Sonnenberg, M. Hada, M. Ehara, K. Toyota, R. Fukuda, J. Hasegawa, M. Ishida, T. Nakajima, Y. Honda, O. Kitao, H. Nakai, T. Vreven, J. A. Montgomery, Jr., J. E. Peralta, F. Ogliaro, M. Bearpark, J. J. Heyd, E. Brothers, K. N. Kudin, V. N. Staroverov, R. Kobayashi, J. Normand, K. Raghavachari, A. Rendell, J. C. Burant, S. S. Iyengar, J. Tomasi, M. Cossi, N. Rega, J. M. Millam, M. Klene, J. E. Knox, J. B. Cross, V. Bakken, C. Adamo, J. Jaramillo, R. Gomperts, R. E. Stratmann, O. Yazyev, A. J. Austin, R. Cammi, C. Pomelli, J. W. Ochterski, R. L. Martin, K. Morokuma, V. G. Zakrzewski, G. A. Voth, P. Salvador, J. J. Dannenberg, S. Dapprich, A. D. Daniels, Ö. Farkas, J. B. Foresman, J. V. Ortiz, J. Cioslowski, and D. J. Fox, Gaussian 09 (Gaussian, Inc., Wallingford CT, 2009).

[37] AIMAll (Version 19.10.12), T. A. Keith, TK Gristmill Software, Overland Park KS, USA, 2019 (aim.tkgristmill.com)

[38] (*a*) L. Tian and C. Feiwu, *J. Comput. Chem*., 2012, **33**, 580−592. (*b*) L. Tian Lu and C. Feiwu, *J. Mol. Graph. Model*., 2012, 38, 314-323.

[39] S. F. Boys and F. Bernardi. *Mol. Phys*., 1970, **19**, 553−566.